Supplementary Information for

Enhancing the brightness of electrically driven single-photon sources using color centers in silicon carbide

*Igor A. Khramtsov, Andrey A. Vyshnevyy, and Dmitry Yu. Fedyanin**

Laboratory of Nanooptics and Plasmonics, Moscow Institute of Physics and Technology, Dolgoprudny 141700, Russian Federation.

*e-mail: dmitry.fedyanin@phystech.edu

SUPPLEMENTARY METHODS

Simulation of the single-photon emitting diode

We performed 2D numerical simulations of the electron and hole transport in the p^+–n–n^+ SiC diode using a steady-state model which comprises the Poisson equation for the electrostatic field, drift-diffusion equations, and carrier continuity equations. The simulations were carried out using the nextnano software (Fig. S1).[S1] The simulation geometry is consistent with that used in Ref. S2. The thickness of the epilayer was 4.9 μm; the substrate thickness was chosen to be 5 μm. The simulation domain was 15 μm wide, which was sufficient to eliminate the influence of lateral boundaries on the charge transport. The top contact was 7.5 μm wide and placed in the left half of the simulation domain, while the bottom contact was 15 μm wide. The p^+ region adjacent to the top contact had a complex doping profile (see Fig. 1 in the manuscript) due to the nonuniformity of dopant distribution obtained by ion implantation and subsequent annealing.[S2] The density of acceptors in the p^+ region was taken uniform and was equal to 10^{19} cm^{-3}, which corresponds to the number of dopants which was activated after implantation of acceptors

($N_{Al} = 5 \times 10^{19}$ cm^{-3}) and subsequent annealing at 1800 °C.[S3] The p region was between the p$^+$ and n regions. The doping profile was modeled using a Gaussian profile with a characteristic width of σ_{Al} = 100 nm (see Fig. 1 in the manuscript). The electron mobilities in the p$^+$, n and n$^+$ regions were equal to 85 cm^2/Vs, 900 cm^2/Vs, 50 cm^2/Vs, respectively. The hole mobilities were 40 cm^2/Vs, 100 cm^2/Vs and 30 cm^2/Vs, respectively.[S4] The carrier lifetime in the epilayer was estimated to be 10 ns, which includes recombination at both bulk and surface traps.[S5] These and other parameters used in the simulations can be found in Table S1.

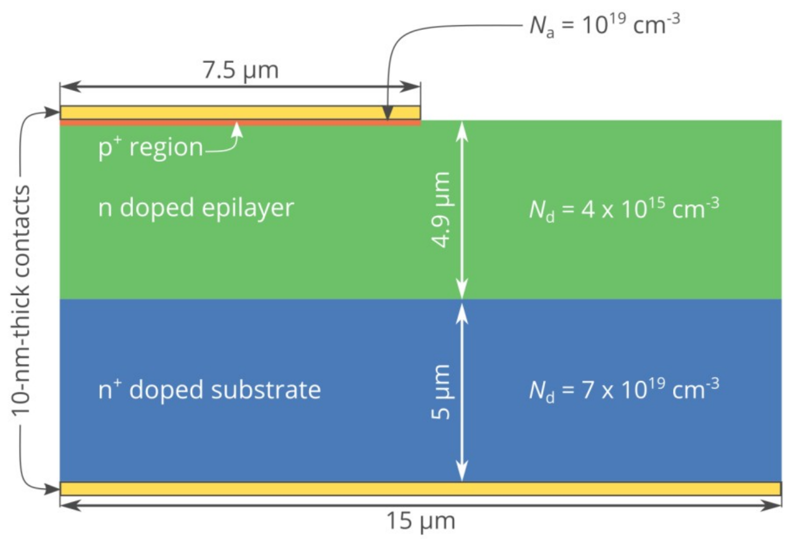

Figure S1. Schematic of the simulation domain.

Table S1. Parameters used in the simulations.

Parameter	Value	Comment
Radiative lifetime of the excited state, τ_r	3.6 ns	Ref. S2
Nonradiative lifetime of the excited state, τ_{nr}	36 ns	Ref. S2
Lifetime of the shelving state τ_s	35 ns	Estimated from $g^{(2)}$ curves
Collection efficiency	1.5%	Estimated from rate curves

Detection efficiency	53%	Ref. S2
Hole capture cross-section by the neutral center, σ_p	5×10^{-15} cm^2	Ref. S6,S7
Dielectric constant, ε	9.78	Ref. S8
Sound velocity, s	1.1×10^{6} cm/s	Ref. S9
Temperature dependence of the electron mobility in the n-type region	extracted from Ref. S4	
DOS effective mass for electrons	$0.77m_0$	Ref. S10, m_0 is the free electron mass
Conductivity effective mass for electrons	$0.36m_0$	Ref. S10, m_0 is the free electron mass
DOS effective mass for holes	$1.0m_0$	Ref. S10, m_0 is the free electron mass
Conductivity effective mass for holes	$1.0m_0$	Ref. S10, m_0 is the free electron mass
Density of activated acceptors in the p^+-type region	10^{19} cm^{-3}	Refs. S2,S3
Density of activated donors (N) in the n^+-type region	7×10^{19} cm^{-3}	Refs. S2,S11
Density of activated donors (N) in the n-type region	4×10^{15} cm^{-3}	Ref. S2
Carrier lifetime in the n-type region	10 ns	Ref. S5
Electron mobility in the p^+-type region	85 cm^2/Vs	Ref. S4
Electron mobility in the n-type region	900 cm^2/Vs	Ref. S4
Electron mobility in the n^+-type region	50 cm^2/Vs	Ref. S4
Hole mobility in the p^+-type region	40 cm^2/Vs	Ref. S4
Hole mobility in the n-type region	100 cm^2/Vs	Ref. S4

Hole mobility in the n^+-type region	30 cm^2/Vs	Ref. S4

Electroluminescence model of the color center with three charge states

Here, we consider a color center in the crystal lattice of silicon carbide which has three charges states (positive, neutral and negative), the neutral charge state has an excited level for electrons and a shelving state (for detail, see Fig. S2).

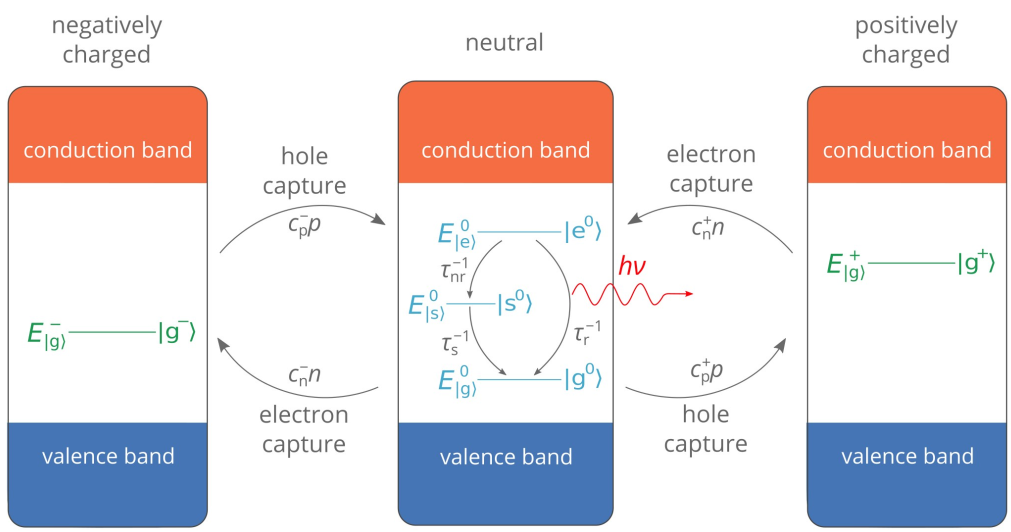

Figure S2. Schematic diagram of the single-photon electroluminescence process for the color center with three charge states. $|e^0>$, $|g^0>$, $|s^0>$ denote the excited, ground and shelving states of the neutrally charged center, respectively. $|g^+>$ and $|g^->$ are the ground states of the color center in the positively and negatively charged charge states. Arrows indicate transitions among different states of the color center. Transition rates are shown next to each arrow.

Following Fedyanin and Agio[12] and neglecting thermal excitations, we can write rate equations for the population of the states of the color center shown in Fig. S2:

$$
\begin{cases}
\dfrac{d n_{\mathrm{e}}}{d\tau} = n_{+} c_{\mathrm{n}}^{+} n + n_{-} c_{\mathrm{p}}^{-} p - \dfrac{n_{\mathrm{e}}}{\tau_{\mathrm{r}}} - \dfrac{n_{\mathrm{e}}}{\tau_{\mathrm{nr}}} \\
\dfrac{d n_{\mathrm{s}}}{d\tau} = \dfrac{n_{\mathrm{e}}}{\tau_{\mathrm{nr}}} - \dfrac{n_{\mathrm{s}}}{\tau_{\mathrm{s}}} \\
\dfrac{d n_{\mathrm{g}}}{d\tau} = \dfrac{n_{\mathrm{e}}}{\tau_{\mathrm{r}}} + \dfrac{n_{\mathrm{s}}}{\tau_{\mathrm{s}}} - n_{\mathrm{g}} c_{\mathrm{p}}^{+} p - n_{\mathrm{g}} c_{\mathrm{n}}^{-} n \\
\dfrac{d n_{+}}{d\tau} = n_{\mathrm{g}} c_{\mathrm{p}}^{+} p - n_{+} c_{\mathrm{n}}^{+} n \\
\dfrac{d n_{-}}{d\tau} = n_{\mathrm{g}} c_{\mathrm{n}}^{-} n - n_{-} c_{\mathrm{p}}^{-} p
\end{cases}
\qquad \text{(S1)}
$$

In this system of equations, n and p are the electron and hole densities in the vicinity of the color center, respectively, n_{e}, n_{s}, and n_{g} are the populations of the excited, shelving and ground states of the neutral defect, and n_{+} and n_{-} are the populations of the positively and negatively charged charge states, respectively. $1/\tau_{\mathrm{r}}$, $1/\tau_{\mathrm{nr}}$, $1/\tau_{\mathrm{s}}$ are the transition rates between the excited, shelving and ground states of the neutral center. c_{n}^{+} and c_{n}^{-} are the electron capture rate constants by the color center in the positively and neutrally charged charge states. c_{p}^{+} and c_{p}^{-} are hole capture rate constants by the color center in the neutrally and negatively charged charge states (see Fig. S2).

Solving equation (S1) in the steady state, we can find the single-photon emission rate:

$$
R = \frac{n_{\mathrm{e}}^{\mathrm{ss}}}{\tau_{\mathrm{r}}} = \left[\tau_{\mathrm{r}} \left(1 + \frac{\tau_{\mathrm{s}}}{\tau_{\mathrm{nr}}} \right) + \frac{1}{c_{\mathrm{p}}^{+} p + c_{\mathrm{n}}^{-} n} \left(1 + \frac{c_{\mathrm{p}}^{+} p}{c_{\mathrm{n}}^{+} n} + \frac{c_{\mathrm{n}}^{-} n}{c_{\mathrm{p}}^{-} p} \right) \left(1 + \frac{\tau_{\mathrm{r}}}{\tau_{\mathrm{nr}}} \right) \right]^{-1} \qquad \text{(S2)}
$$

Here $n_{\mathrm{e}}^{\mathrm{ss}}$ is the steady-state population of the excited state $|e^{0}\rangle$ of the neutrally charged center.

This model can be easily reduced to the 2-charge-states model presented in the main text by putting $c_{\mathrm{n}}^{-} = 0$ in equation (S1). In other words, transitions from the neutrally charged state to the negatively charged state are forbidden. Similarly, one can consider a color center with neutral and negatively charged charge states by putting $c_{\mathrm{p}}^{+} = 0$ in equation (S1).

As discussed in the main text, the capture rate constants c_n^-, c_p^-, c_n^+, c_p^- are the products of the carrier capture cross-sections and the corresponding thermal velocities. We can assume the electron and hole capture cross-sections by the neutrally charged center to be roughly equal to each other, while the hole capture cross-section by the negatively charged center can be estimated in the same way as the electron capture cross-section by the positively charged center (for details, see the main text).

Figure S3 shows the comparison between the developed 3-charge-states model and the 2-charge-states model from the main text. To apply the 3-charge-states model to the Si_C-SF center, we assume that a negatively charged charge state of this center exists. It can be seen that the photon emission rate for the color center with three charge states is slightly higher than for the color center with two charge states, and the characteristic time of the $g^{(2)}$ function is lower due to the decreased "recharge" time of the color center.

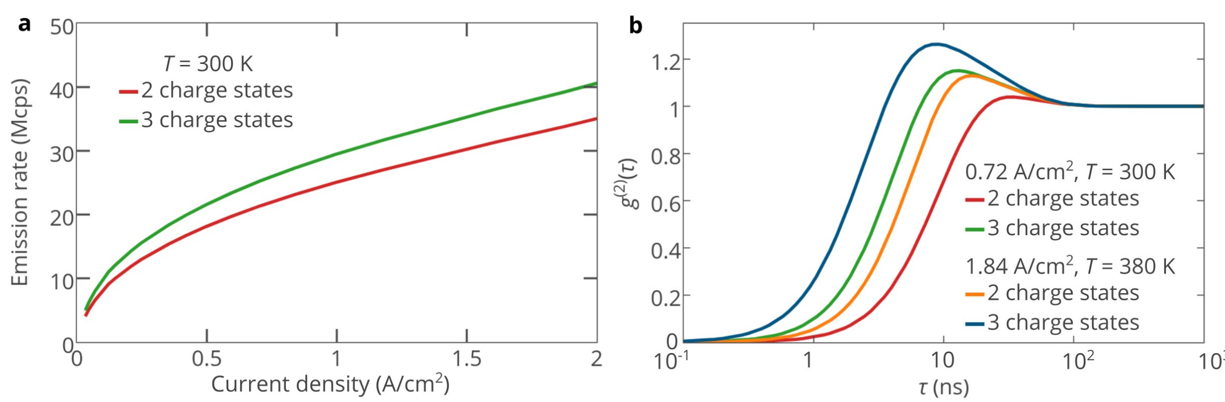

Figure S3. (a) Photon emission rate versus pump current for the 2-charge-states and 3-charge-states models. (b) $g^{(2)}$ curves for two different models. The simulations are performed for the color center at point 2 in Figure 3a in the main text.

REFERENCES

S1. Birner, S. *et al.* nextnano: General purpose 3-D simulations. *IEEE Trans. Electron Dev.* **54,** 2137–2142 (2007).

S2. Lohrmann, A. *et al.* Single-photon emitting diode in silicon carbide. *Nat. Commun.* **6,** 7783 (2015).

S3. Zhe, C. F. *Silicon Carbide: Materials, Processing & Devices*. (CRC Press, 2003).

S4. Mnatsakanov, T. T., Levinshtein, M. E., Pomortseva, L. I. & Yurkov, S. N. Carrier mobility model for simulation of SiC-based electronic devices. *Semicond. Sci. Technol.* **17,** 974–977 (2002).

S5. Nakayama, K. *et al.* Characteristics of a 4H-SiC Pin Diode With Carbon Implantation/Thermal Oxidation. *IEEE Trans. Electron Dev.* **59,** 895–901 (2012).

S6. Friedrichs, P., Kimoto, T., Ley, L. & Pensl, G. *Silicon Carbide: Volume 1: Growth, Defects, and Novel Applications*. (Wiley-VCH, 2011).

S7. Claeys, C. & Simoen, E. *Radiation Effects in Advanced Semiconductor Materials and Devices*. (Springer, 2002).

S8. Persson, C., Lindefelt, U. & Sernelius, B. E. Doping-induced effects on the band structure in n-type 3C−, 2H−, 4H−, 6H−SiC, and Si. *Phys. Rev. B* **60,** 16479–16493 (1999).

S9. Chinone, Y., Ezaki, S., Fujita, F. & Matsumoto, K. Applications of High Purity SiC Prepared by Chemical Vapor Deposition. in *Springer Proceedings in Physics* **43,** 198–206 (1989).

S10. Son, N. T. *et al.* Electron effective masses in 4H SiC. *Appl. Phys. Lett.* **66,** 1074–1076 (1995).

S11. Cree Silicon Carbide Substrates and Epitaxy. Available at: https://www.macrogroup.ru/sites/default/files/uploads/catalog/silovaya_electronika/CREE/matcatalog.pdf. (Accessed: 4th January 2018)

S12. Fedyanin, D. Yu. & Agio, M. Ultrabright single-photon source on diamond with electrical pumping at room and high temperatures. *New J. Phys.* **18,** 073012 (2016).